SAND2017-12910C

Evaluating the Performance of Fasteners Subjected to Multiple Loadings and Loadings Rates and Identifying Sensitivities of the Modeling Process

John P. Mersch[1] and Jeffrey A. Smith[2]
Sandia National Laboratories, Albuquerque, NM, 87185

Evan P. Johnson[3]
Sandia National Laboratories, Albuquerque, NM, 87185

and

Thomas Bosiljevac[4]
Sandia National Laboratories, Albuquerque, NM, 87185

This study details a complimentary testing and finite element analysis effort to model threaded fasteners subjected to multiple loadings and loading rates while identifying modeling sensitivities that impact this process. NAS1352-06-6P fasteners were tested in tension at quasistatic loading rates and tension and shear at dynamic loading rates. The quasistatic tension tests provided calibration and validation data for constitutive model fitting, but this process was complicated by the difference in the conventional (global) and novel (local) displacement measurements. The consequences of these differences are investigated in detail by obtaining calibrated models from both displacement measurements and assessing their performance when extended to the dynamic tension and shear applications. Common quantities of interest are explored, including failure load, time-to-failure, and displacement-at-failure. Finally, the mesh sensitivities of both dynamic analysis models are investigated to assess robustness and inform modeling fidelity. This study is performed in the context of applying these fastener models into large-scale, full system finite element analyses of complex structures, and therefore the models chosen are relatively basic to accommodate this desire and reflect typical modeling approaches. The quasistatic tension results reveal the sensitivity and importance of displacement measurement techniques in the testing procedure, especially when performing experiments involving multiple components that inhibit local specimen measurements. Additional compliance from test fixturing and load frames have an increasingly significant effect on displacement data as the measurement becomes more global, and models must necessarily capture these effects to accurately reproduce the test data. Analysis difficulties were also discovered in the modeling of shear loadings, as the results were very sensitive to mesh discretization, further complicating the ability to analyze joints subjected to diverse loadings. These variables can significantly contribute to the error and uncertainty associated with the model, and this study begins to quantify this behavior and provide guidance on mitigating these effects. When attempting to capture multiple loadings and loading rates in fasteners through simulation, it becomes necessary to thoroughly exercise and explore test and analysis procedures to ensure the final model is appropriate for the desired application.

[1] R&D S&E Mechanical Engineering, Component Science & Mechanics, PO Box 5800, MS0346
[2] R&D S&E Mechanical Engineering, Component Science & Mechanics, PO Box 5800, MS0346
[3] R&D S&E Mechanical Engineering, Advanced Munitions & Mechanical Systems, PO Box 5800, MS1183
[4] R&D S&E Mechanical Engineering, Experimental Environment Simulation, PO Box 5800, MS0557

Nomenclature

DVRT	=	Differential Variable Reluctance Transducer
eqps	=	equivalent plastic strain
MLEP	=	multi-linear elastic-plastic
K	=	amplitude of pulse in Gs
t	=	time
τ	=	pulse duration

I. Introduction

Finite element analysis of complex, full system structures is increasingly relied upon to inform engineering decision-making, and creating robust, predictive models of all components in the assembly maximizes confidence in the analysis results. Threaded fasteners are often one of the integral parts in these structures, and many times the performance of these joints can be critical to the overall structural integrity of a component. It thus becomes desirable to have fastener models capable of predicting the behavior of these joints in diverse environments while limiting their fidelity to accommodate the simulation of the larger structure. Unfortunately, the typical process for obtaining these reduced order fastener models lacks robustness and is plagued with pitfalls that can lead to undesired results. The calibration process is the foundation of model performance, but each test measurement only provides validation at a single point in the engineering structure. Without measurements at multiple locations of the test apparatus, the quality of the calibration cannot be further evaluated and is subject to increased error. Additional uncertainties arise when these models are extended beyond their calibrated environments (i.e. to different loadings and loading rates) and asked to predict performance, as the model parameters may be limited by the desired application and no longer sufficient to capture the relevant mechanics.

The present study is an extension of work previously presented[1], where a complimentary testing and finite element analysis effort was conducted to model threaded fasteners subjected to tensile loadings at quasistatic and dynamic loading rates. A thorough literature search was performed for that study on various modeling approaches for fasteners, including detailed three-dimensional models with threads[2-7], a "plug" approach (fastener head and shank, no threads)[8-10], and various other simplified approaches[11, 12]. The present study focuses less on the effects of a simplified modeling approach, and instead identifies, examines, and quantifies many of the sensitivities that effect the testing-calibrating-modeling process.

The testing of fasteners is typically application specific, and motivated by obtaining the behavior of the *joint*. Many recent studies were found that specifically investigated the behavior of composite bolted joints, motivated by increasing the understanding of their performance in aircraft applications. Qin et. al.[13] performed an experimental and numerical analysis effort to better understand the failure of double-lap composite joints fastened by both countersunk and protruding head fasteners. Stocchi et. al.[14] conducted a similar testing and analysis study on single lap composite bolted joints, identifying distinct stages throughout quasistatic shear loading. Studies of this nature, however, are not intended to characterize the independent behavior of the fastener, and attempting to extend these fastener tests and/or constitutive models to other applications may prove difficult. Fransplass et. al.[15-17] have performed more isolated fastener testing on threaded rods at quasistatic and dynamic loading rates, creating novel test fixtures to load the rod at 45° and investigating failure prediction at 15° incremental loadings in their latest paper. However, their inability to predict the compliance and displacements of the test data may leave doubt in the further application of these constitutive models. Unless the displacements are correctly captured throughout the model, any calibration of fastener properties will necessarily include behavior from the other components/fixtures included in the test and the model will be less robust in other applications.

The overall displacement of the fastener/joint is an important quantity of interest, as it is analogous to energy absorption and a key property of failure. This quantity of interest is experimentally investigated in Egan et.al.[18], where they studied the behavior and failure of bolted composite joints resembling aircraft structure applications. Energy absorption is one of the main topics of this paper, and the authors remark, "A crucial role of an airframe is to absorb energy in an impact situation, improving survivability". Since this quantity is critical to the prediction of failure, it is important to understand its provenance and progression through the testing-calibration-modeling cycle.

This current study further details the testing of NAS1352-06-6P fasteners in tension at quasistatic loading rates and tension and shear at dynamic loading rates. Elastic-plastic constitutive models for the fastener are calibrated to the quasistatic tension data and then extended to the dynamic applications to evaluate their ability to predict failure. The fastener is modeled as a "plug" of material, where the fastener head and shank are included, but there is no explicit modeling of the threads. This reduced order technique is motivated by the ability to incorporate a similar fastener

modeling approach into a large-scale, full system analysis of a complex structure where many fasteners are present but are a small part of the entire model.

The quasistatic tension tests were equipped with multiple displacement measurement techniques to better understand the compliance of the test setup and ultimately the load-displacement response and energy absorption of the fastener/joint. The first displacement measurement was obtained from the stroke of the test machine, which is sometimes used as the data authority for fastener testing. The second measurement was obtained from a more novel approach, where DVRTs locally measured the relative displacement of the bushings holding the fastener. The results of these measurements were very different, motivating an investigation into the possible error associated between analysis models calibrated to these data. Common quantities of interest are evaluated in this context, including failure load, time-to-failure, and displacement-at-failure. The plug modeling approach is also further assessed by performing a mesh sensitivity study to understand and quantify the ability of this approach to predict failure when element count and size are extremely limited.

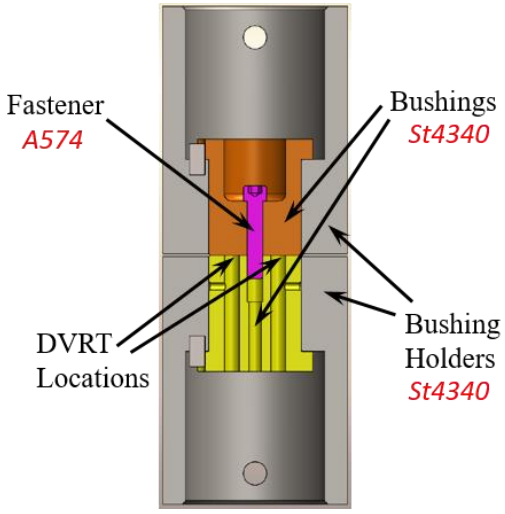

Figure 1. Quasistatic Tension Test Setup

II. Test Setups

Three sets of tests were performed on NAS1352-06-6P[19] fasteners to evaluate their performance in tension at quasistatic loading rates and tension and shear at dynamic loading rates. The three unique test setups are described in the following sections. The tension tests have been previously documented[1], but a similar summary is provided in this paper to consolidate information for the reader.

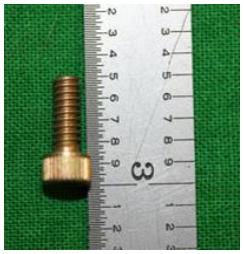

Figure 2. NAS1352-06-6P Fastener

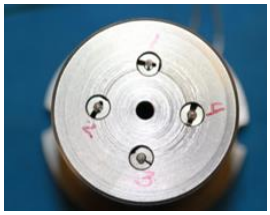

Figure 3. DVRT Locations

A. Quasistatic Testing

The quasistatic tension test apparatus is shown in Figure 1 and is composed of the 4340 steel bushing holders, 4340 steel bushings, and NAS1352-06-6P A574 steel fastener (Figure 2). Displacement data for each quasistatic test was collected by four DVRTs (Figure 3) located 0.75 in (19.1 mm) from the axis of the fixture which measure the gap between the top and bottom bushings. Tests were performed on both preloaded fasteners torqued to 20 in-lb (2.26 N-m) and non-preloaded fasteners (hand tightened).

B. Dynamic Testing

The dynamic tension and shear test setups are shown in Figure 4 and Figure 5, respectively. The dynamic tension test apparatus includes the Al6061-T6 fixture base, SS304L fixture lid, A36 steel 1.0 lb (0.454 kg) tensile mass, 4340 hardened steel bushing, and steel fastener, and the dynamic shear test apparatus includes the 4340 steel fixture base, 4340 steel shear masses (sliding weight, 0.6 lbs), 4340 hardened steel bushings, grade 8 black oxide shoulder bolts, and steel fastener.

To create a dynamic loading scenario, the test fixtures were bolted to the carriage of a bungee accelerated drop table (see Figure 6). When the drop table carriage impacts the reaction mass the fastener experiences a dynamic loading caused by the acceleration of the tensile mass (or sliding weight for the shear apparatus). Depending on the impact magnitude the screw is unchanged, loses preload, or fails catastrophically, where a catastrophic failure was defined as the screw being pulled into two separate pieces.

Endevco model 7270 and 7274 piezoresistive accelerometers were used to measure the acceleration on the carriage, test fixture, and mass. All tests were performed with the fasteners preloaded to 22 in-lb (2.49 N-m). The main objective was to determine the force at which the screw catastrophically fails while varying the shape of the

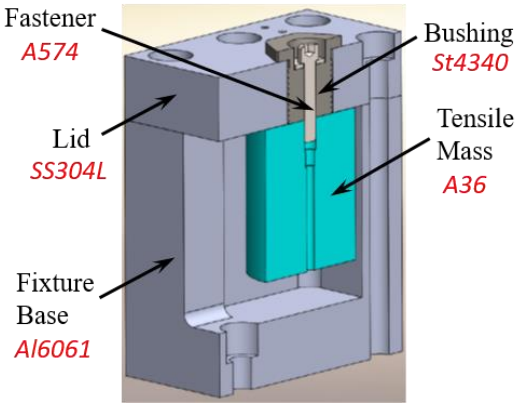

Figure 4. Dynamic Tension Test Apparatus

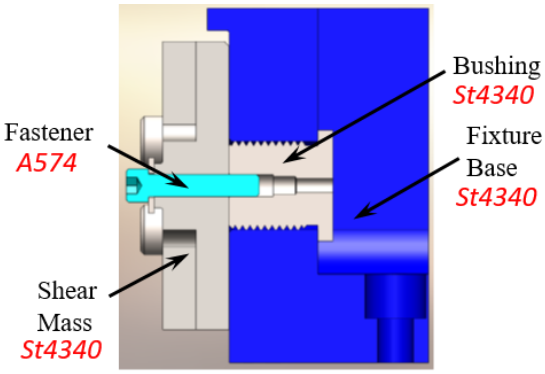

Figure 5. Dynamic Shear Test Apparatus

pulse acceleration. Pulse levels were chosen to span the entire range of the drop table capability. Approximately four fasteners were tested at each velocity level with the intent of bracketing the failure point within those tests.

III. Analysis Models

Finite element analysis models were constructed for each of the three test setups and are described in the following sections. Again, the details of the tension analysis models are previously documented[1], but included here for completeness.

A. Quasistatic

One-quarter of the quasistatic tension setup is modeled utilizing symmetry of the design and is shown in Figure 7. The bushings and bushing holders are modeled as elastic bodies with representative 4340 steel properties, and the fastener is modeled with a multi-linear elastic-plastic (MLEP) model which will be described in detail in a later section. A prescribed displacement is applied to the top of the bushing holder, and displacements are analytically measured at the DVRT locations to enable direct comparisons to the test results. Simulations are performed using the implicit module of the code Sierra/SM[20] and 8-node**,** uniform gradient hexahedra elements are used for all geometry. Material properties for the fastener and 4340 steel are provided in Table 1.

B. Dynamic

One-half model symmetry is utilized for both dynamic testing setups, which are shown in Figure 8 and Figure 9. The 4340 steel blocks are modeled with the Johnson-Cook constitutive model[21], the Al6061 and SS304L blocks are modeled using an elastic-plastic model with piecewise-linear hardening, and the A36 is modeled with power-law hardening. Material properties for the dynamic simulations are provided in Table 2, and the MLEP x-y pairs are included in Appendix A. Simulations are performed using the explicit module of the code Sierra/SM and 8-node**,** uniform gradient hexahedra elements are used for all geometry.

The drop table tests are simulated by prescribing a pulse acceleration to reproduce the test loading. The pulse takes the form of,

$$K \sin^2\left(\frac{\pi t}{\tau}\right) \qquad (1)$$

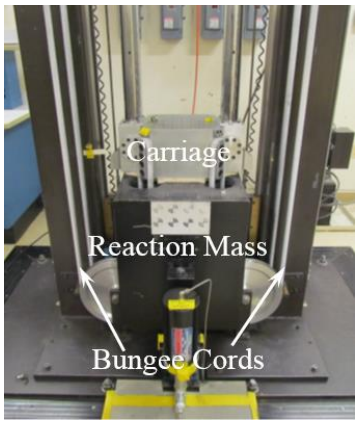

Figure 6. Drop Table Experimental Setup

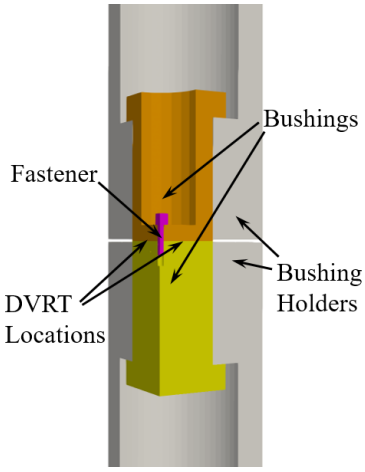

Figure 7. Quasistatic Tension Model

where K is the pulse amplitude in in/s^2, t is the time after impact, and τ is the baseline pulse duration in seconds. An example of a test pulse and the analysis approximation are shown in Figure 10. In some cases, the beginning and end of the test pulse was ambiguous, and the duration of the analysis pulse was fit to best represent the test data. This prescribed acceleration is analytically applied to the bottom of the test fixture where it attaches to the drop table carriage during testing.

Table 1. Quasistatic Analysis Material Properties

Quasistatic Material Properties	St4340	Fastener (DVRT)	Fastener (Stroke)
Density, ρ (snails/in^3)	0.0007133	0.000725	0.000725
Young's Modulus, E (psi)	3.04E+07	2.85E+07	5.2E+0.6
Poisson's Ratio, ν	0.3	0.3	0.3
Yield Stress, σ_y (psi)	-	145000	160000

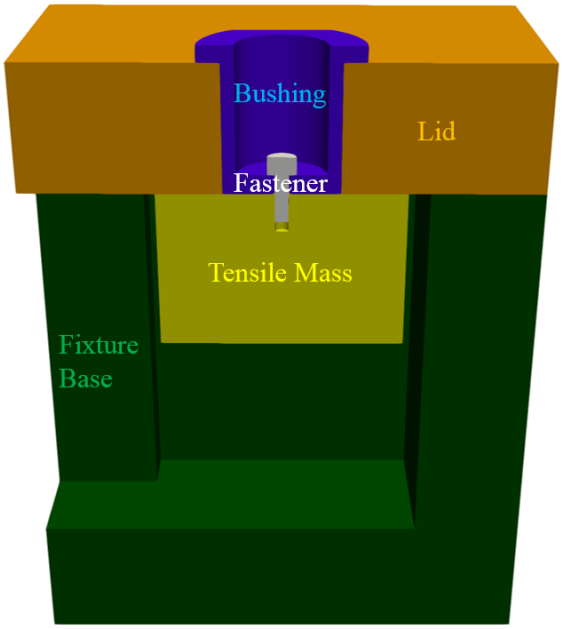

Figure 8. Dynamic Tension Analysis Model

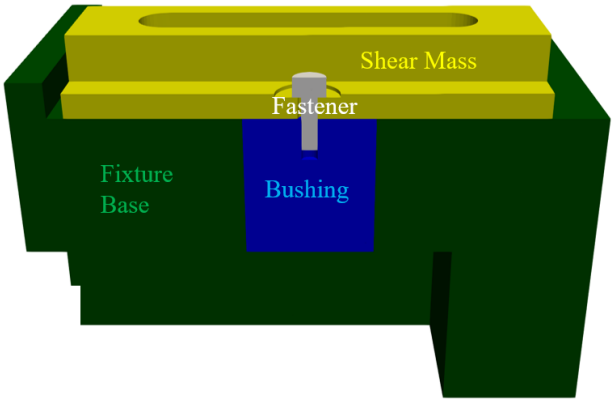

Figure 9. Dynamic Shear Analysis Model*

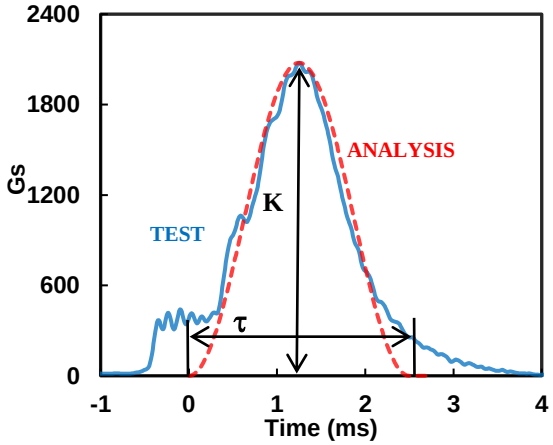

Figure 10. Example of Drop Table Pulse

*Note that the shoulder bolts were omitted in the analysis model and not included in any simulations

Table 2. Dynamic Analysis Material Properties

Dynamic Material Properties		Al6061	SS304L	St4340	A36	Fastener
Basic	Density, ρ (snails/in^3)	0.000254	0.000732	*0.0007352*†	0.000724	0.000725
	Young's Modulus, E (psi)	1.00E+07	2.80E+07	3.04E+07	3.00E+07	2.85E+07
	Poisson's Ratio, ν	0.3	0.3	0.3	0.3	0.33
	Yield Stress, σ_y (psi)	45000	36200	149000	37400	150000
MLEP	Beta	1	1	-	-	1
	Critical Tearing Parameter, t_p	1.586	12.04	-	-	-
	Critical Crack Opening Strain	0.1	0.1	-	-	-
Johnson-Cook	Hardening Constant, B (psi)	-	-	157800	-	-
	Hardening Exponent, n	-	-	0.26	-	-
	Density*Specific Heat, ρC_v (lb/in^2.K)	-	-	298	-	-
	Rate Constant (C)	-	-	0.014	-	-
	Thermal Exponent (m)	-	-	1.03	-	-
	Reference Temperature (T_{ref})	-	-	298	-	-
	Melting Temperature (T_{melt})	-	-	2768	-	-
Powerlaw Hardening	Hardening Constant, A (psi)	-	-	-	700000	-
	Hardening Exponent, m	-	-	-	0.38	-
	Luders strain	-	-	-	0.0057	-

C. Fastener Modeling

The fastener is modeled as a "plug" of hexahedra elements, which incorporates the fastener head and shank (without threads) and models the threaded connection with tied contact. The plug modeling approach is illustrated in Figure 11. A MLEP constitutive model is used for all fastener elements and a death criterion is defined to model failure by approximating the maximum equivalent plastic strain (eqps) that reproduces the displacement-to-failure observed in this quasistatic tension test. The diameter of the modeled fastener is set equal to the "tensile threaded stress area" defined in ASMEB1.1-2003[22]. Simulations were initially conducted with 16 elements through the diameter of the fastener. This is beyond the limit of the application of interest (4-6 elements through the diameter), but a higher fidelity was chosen for effective calibration. Mesh sensitivity was later investigated to provide guidance for reduced order fastener modeling relevant to the application.

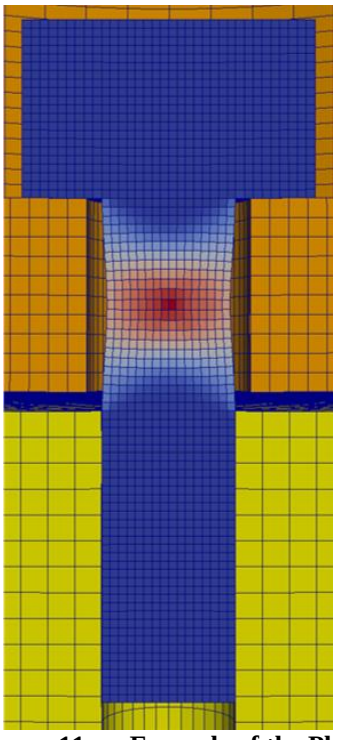

Figure 11. Example of the Plug

IV. Calibration

One of the main objectives of this study was to evaluate the performance of constitutive model properties obtained from quasistatic tension in different strain rate and load environments. Therefore, surrogate material properties for the fastener were obtained through calibration routines that adjusted the piece-wise linear hardening curve to best reproduce the load-displacement curve from analogous test data. This calibrated model was then extended to the dynamic tension

†density was modified for dynamic shear test fixtures to match mass (real test fixtures have holes).

and dynamic shear applications to assess the model's ability to predict failure in different loading conditions.

D. Model Calibration

Two displacement measurement techniques were incorporated in the quasistatic tension tests – a local measurement from DVRTs monitoring the relative displacement of the bushings and the global stroke measurement. An example of the typical raw load-displacement curves obtained from the DVRT and stroke test measurements are shown in Figure 13 with the smoothed and shifted data shown in Figure 14. The DVRT and stroke responses in the elastic region are quite different, and the final displacement of the stroke is approximately 60% larger than the DVRT in the raw data and 25% larger in the smoothed data. These differences – which have direct consequences on the energy absorption of the joint – must be resolved during the calibration process to ensure an accurate and robust model.

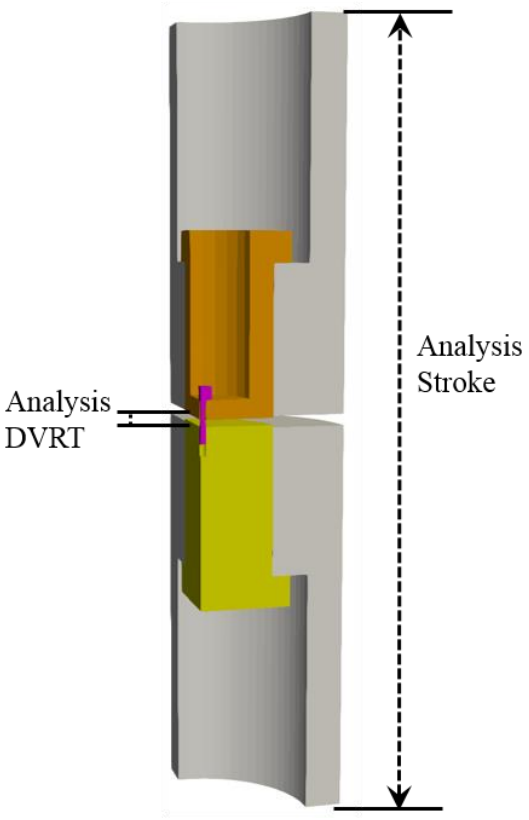

Figure 12. Analytical Measurements of DVRT and Stroke

Fitting the MLEP constitutive model is a complicated multi-step process. Full documentation of the general procedure is documented in a Sandia Report[23], but a brief, application-specific description is also included here. The full quasistatic tension analysis model is used to calibrate. Displacements are extracted from the bushings at the virtual DVRT location to reproduce the DVRT test measurement, and displacement is also output at the top of the bushing holder to reproduce the stroke measurement (see Figure 12. Note that the displacement magnitudes in the figure have been increased to better highlight the measurements incorporated in the simulations.). The A574 Young's Modulus which was used for the DVRT calibration was obtained from another analyst, but it was confirmed that A574 is a medium carbon alloy steel[24] and that this value falls within typical values for these types of alloys[25,26]. However, the error between the elastic region of the stroke data and this Young's Modulus value was too large; therefore, simulations were conducted with various modulus values until an acceptable reproduction of the elastic region was obtained. Yield stress values were then chosen to best accommodate the hardening curve calibration.

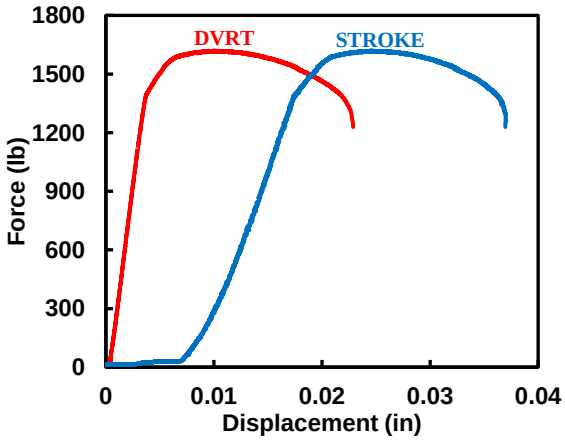

Figure 13. Quasistatic Tension Test Results – DVRT and Stroke Measurements

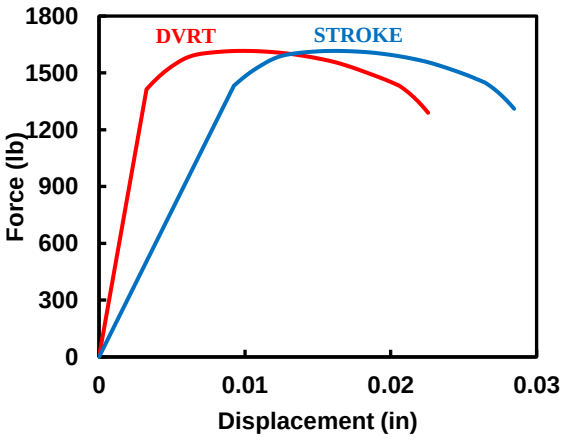

Figure 14. Quasistatic Tension Test Results – DVRT and Stroke Measurements (Shifted, Smoothed)

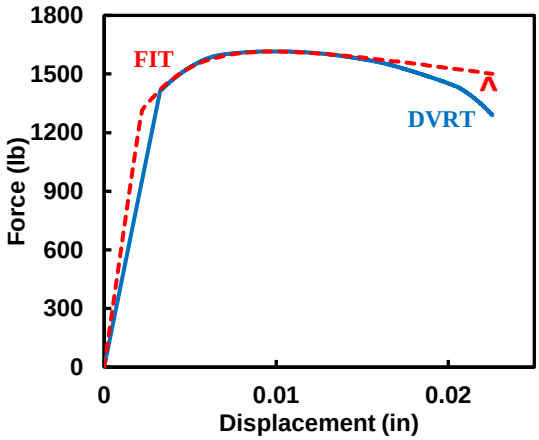

Figure 15. Quasistatic Tension Analysis Model Calibration – DVRT

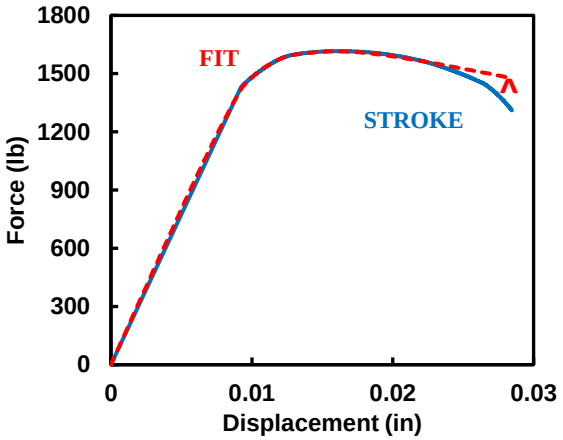

Figure 16. Quasistatic Tension Analysis Model Calibration – Stroke

The results of the DVRT and stroke calibrations are shown in Figure 15 and Figure 16, respectively, elastic properties are provided in Table 1, and hardening curves are provided in Figure 17. The triangular marks seen in Figure 15 and Figure 16 denote the points at which the eqps failure criterion (provided in Appendix A) fails the fastener, which correspond to the displacements at failure seen in the respective tests. Both calibrated models reproduce the test data very well, especially up to peak load. However, note that the A574 Young's Modulus was reduced by a factor of five to capture the elastic behavior of the stroke measurement. Additional compliance significantly contributes to the stroke displacement and thus the measurement is no longer representative of the fastener behavior. Unless all of the compliance associated with this measurement can be reproduced analytically, the behavior of the fastener cannot be isolated and the effects of the joint and machine are integrated into the calibration.

The differences in these measurements motivated the analysts to determine where in the test setup the additional compliance manifests. Is it material compliance in the test fixtures? Tolerances between the bushings and bushing holder? Or is it the inherent compliance of the test machine? Some insight to this question can be gained by comparing the displacement outputs of the DVRT and stroke from the quasistatic tension analysis, which are plotted in Figure 18. These two measurements are nearly identical in the analysis, indicating that the main source of the additional compliance is likely outside of the test fixtures all together. These results also indicate that the analysis isn't accurately reproducing both displacement measurements – there is a large difference in the DVRT and stroke in the test results, but they are essentially equal in the analysis. Given that the literature Young's Modulus reasonably captures the elastic region of the DVRT, this analytical measurement is likely more accurate, and the

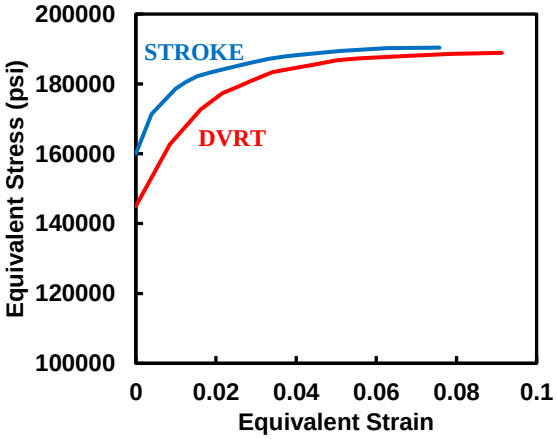

Figure 17. Hardening Curves for DVRT and Stroke from MLEP Calibration

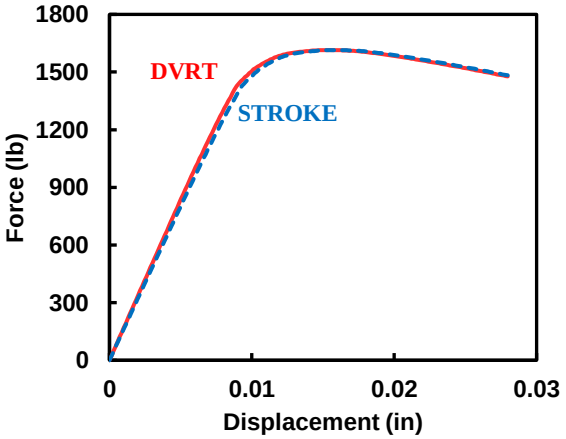

Figure 18. Comparison of DVRT and Stroke Displacement Measurements from Analysis

compliance from the test machine is not captured in the current analysis model. Further, more detailed analyses that included additional testing components yielded similar results[27]. Although this is likely enough evidence to dismiss the stroke calibration, some testing series do not examine the test with this level of detail, and accept the stroke measurement (or a similar global measurement) as the data authority. Therefore, this stroke calibration will be extended to other applications and compared to the DVRT calibration to evaluate its performance and assess the differences.

V. Model Extension

After the models were calibrated, they were applied to predict the dynamic tension and shear measurements to assess the differences associated with the DVRT and stroke calibrations, evaluate how well the DVRT fit reproduces the test data, and investigate the mesh sensitivities associated with each loading condition. Test data was obtained from drop table tests which provided the failure load of the fastener for a set of pulse durations (see Figure 10), which nominally span strain rates of 100ε/s-1000ε/s for this testing series. Analysis failure curves were obtained by conducting simulations at fixed pulse durations while increasing the peak acceleration magnitude by 25 G increments until complete cross-section failure occurred. For both test and analysis curves, anything below the curve represents an intact fastener and anything above represents complete cross-section failure.

A. Mesh Sensitivities

The results detailed in the calibration section were obtained from simulations with 16 elements through the diameter of the fastener. However, this type of fidelity is typically not attainable for fasteners in system models of complex structures where element size has a large influence on the length of the analysis. Therefore, the mesh sensitivity of the dynamic tension and shear applications were evaluated to inform reduced order fastener modeling and ensure both calibrations were evaluated with mesh converged analyses.

Analyses of the dynamic tension model (with the DVRT calibrated fastener) were conducted for 4, 8, 12, and 16 elements through the diameter of the fastener, and the results are shown in Figure 19 where pulse duration is plotted on the x-axis and the peak acceleration (in Gs) is plotted on the y-axis. The analyses suggest that the tension application is mostly mesh insensitive, as the failure loads of the 4-element mesh are nearly identical to the 16-element mesh, differing by less than 7% for all pulse durations. Furthermore, this difference in failure load can be partially attributed to the reduction in cross-sectional area of the 4-element fastener. As less elements are incorporated, the modeled cross-section becomes smaller, and the load carrying capacity of the fastener decreases. In this case, the area of the cross section is reduced from 0.009077 in^2 to 0.008680 in^2 (a 4% reduction) when going from 16 to 4 elements through the diameter, and the loads vary in a similar way for pulse durations larger than 1.0 ms.

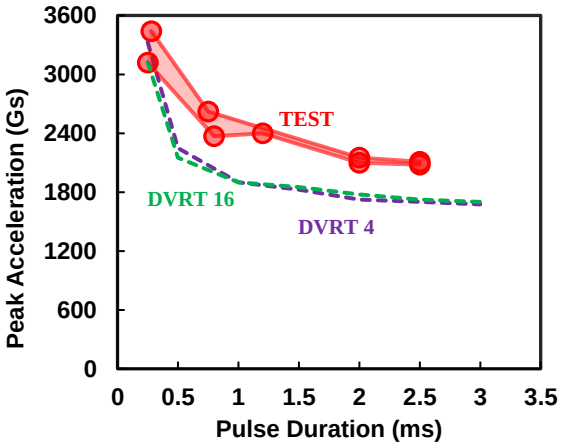

Figure 19. Dynamic Tension Test and Analysis Results – Mesh Sensitivity

Analyses of the dynamic shear model (with the DVRT calibrated fastener) were conducted for 4, 8, 12, and 16, 20, and 24 elements through the diameter of the fastener, and the results are shown in Figure 20, with examples of the meshes shown in Figure 21.

For the shear case, the model is extremely mesh sensitive, as failure loads differ by at least 1100 Gs from the 4 to 24 element models, and percent differences are at least approximately 50% for all pulse durations.

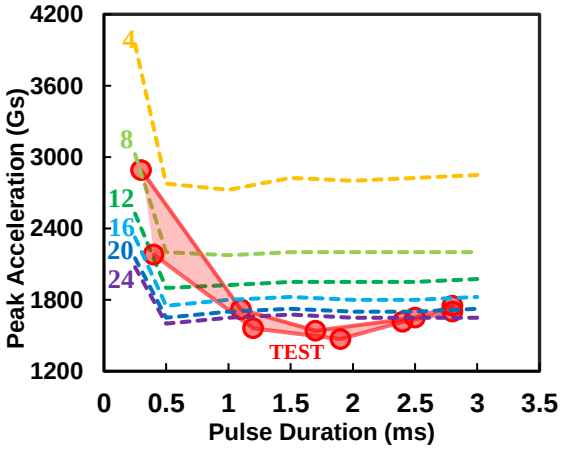

Figure 20. Dynamic Shear Test and Analysis Results – Mesh Sensitivity

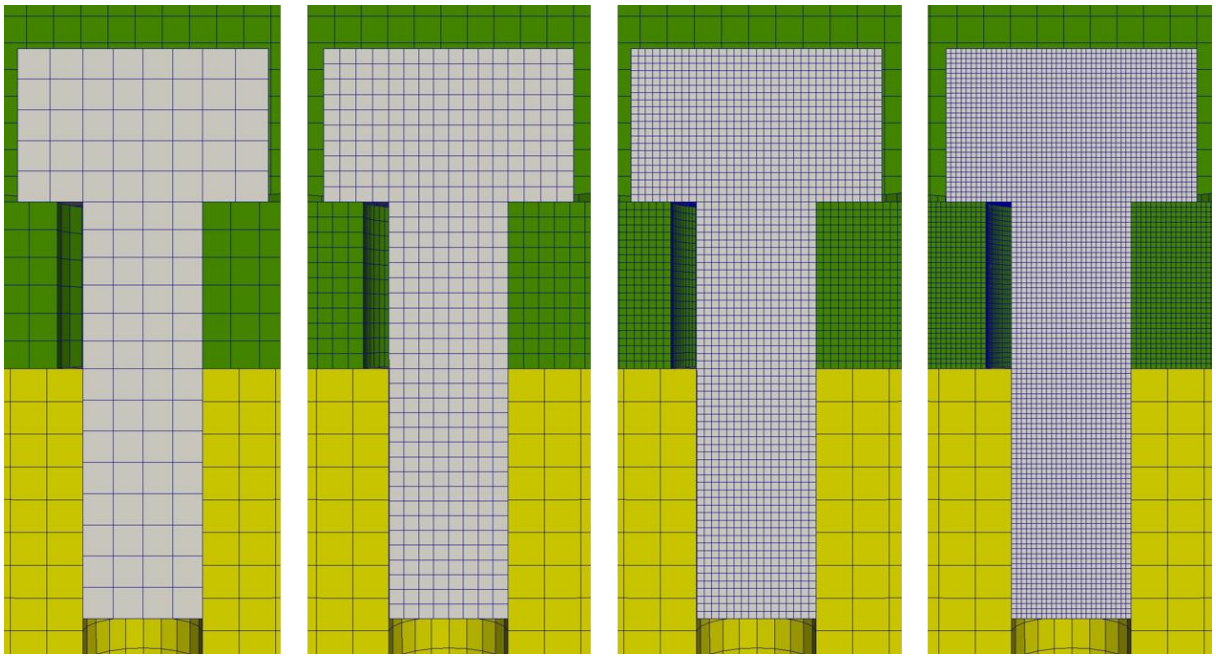

Figure 21. Meshes in the Sensitivity Study (4, 8, 16, and 24)

Furthermore, all analyses have some regions which are nonconservative compared to test data, and the coarser meshes miss the failure loads by up to 1250 Gs, an 80% overprediction. Note that the meshes in Figure 21 were refined for the shear mass, as this discretization is also important to capture the local shear loading in the fastener.

This difference in the sensitivities of the two models consequently makes it difficult to accurately capture both behaviors with the same mesh, especially when element size is limited. An analyst could simply "shift" the hardening curve down in an attempt to better capture shear failure with a coarsely meshed fastener, but this would also shift the already conservative tensile failure prediction down, and the associated errors would likely be unacceptable. Without additional modification, the best current strategy would be to conduct a mesh sensitivity on the component analysis model of interest, and quantify the errors associated with the reduced order approximation.

B. Calibration Sensitivities

The calibrations of the DVRT and stroke detailed in the previous sections were extended to the dynamic tension analyses with mesh converged discretizations to explore the range of results an analyst could obtain for common quantities of interest, including failure load, displacement-at-failure, and time-to-failure.

Both calibrations reasonably reproduce the test results, but consistently underpredict the failure loads observed in testing. However, previous research[1] suggests that this may largely be due to strain rate effects that are not reflected in the strain rate independent constitutive models used in these analyses.

A comparison of the DVRT and stroke analyses reveals that the calibrations yield similar results, but the failure loads deviate between 0.5 and 1.5 ms pulse durations, where there is up to a 17% difference. The cause of this difference is unknown, but one possible explanation is that the relative difference in the Young's Moduli for the DVRT and stroke calibrations are leading to differences in wave propagation that influence the failure loads at certain pulse durations.

The time-to-failure for the fastener was also investigated for each of these approaches, and is summarized in Table 3. For this set of analyses, both models were run for the same pulse (same duration, peak acceleration) which was determined by choosing an

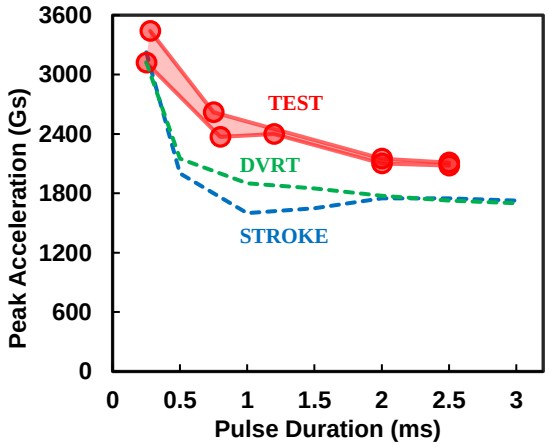

Figure 22. Dynamic Tension Results – Test & Analysis (16 Elements Through Diameter)

Table 3. Summary of Dynamic Tension Analysis Results

Analysis Inputs		DVRT		Stroke		Percent Difference	
Pulse Duration (ms)	Peak Accel (Gs)	Failure Time (ms)	Disp to Fail (in)	Failure Time (ms)	Disp to Fail (in)	Failure Time (%)	Disp to Fail (%)
0.25	3225	0.352	0.0177	0.4	0.0208	12.77%	16.10%
0.5	2150	0.489	0.0176	0.451	0.0207	8.09%	16.19%
1	1900	0.8	0.0172	0.632	0.0208	23.46%	18.95%
1.5	1850	1.11	0.0173	0.864	0.0207	24.92%	17.89%
2	1775	1.37	0.0172	1.27	0.0207	7.58%	18.47%
2.5	1750	1.62	0.0172	1.74	0.0207	7.14%	18.47%
3	1725	1.878	0.0172	1.95	0.0207	3.76%	18.47%

acceleration from the previous study which would fail both fastener models. The results of this study reveal that time-to-failure can vary by as much as 20%, and it varies the most at the same pulse durations where failure load most varied, suggesting that these quantities may be correlated.

Lastly, displacement-to-failure was obtained from both sets of analyses and is also included in Table 3. Unsurprisingly, the quantities are essentially constant through the span of pulse durations (this is a strain-rate independent model), varying by approximately 20%. While this is less than the quantities differed in the quasistatic tension test/analysis, the gage length of the dynamic application was shorter than the quasistatic application (0.20 in to 0.15 in), so this result is expected.

A similar process was repeated for the dynamic shear analyses, and the failure curves from the DVRT and stroke calibrations are compared to the test data in Figure 23. The failure loads for this case tend to vary more than the analogous comparisons for dynamic tension. The failure loads are consistently 300 Gs (~20%) different, and the DVRT failure loads for some pulse durations are nonconservative compared to the test data. This result is more troublesome when considering strain-rate effects have been neglected in the constitutive models, as this would further increase the failure loads and make the results increasingly nonconservative. The time-to-failure of these models also varies more in the shear application, as the percent differences are consistently 20% for all pulse durations larger than 1.0 ms and can be as high as 32%. The full results from these analyses are summarized in Table 4.

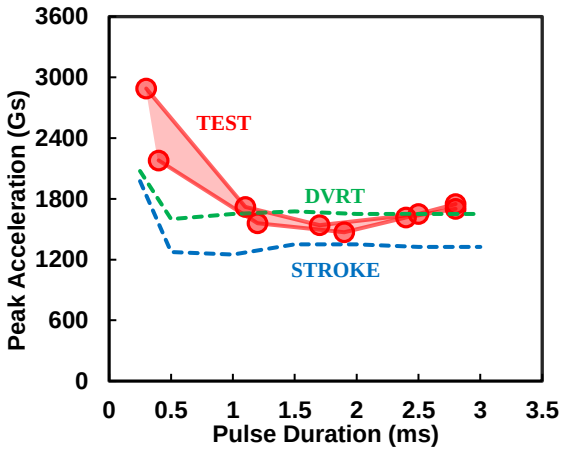

Figure 23. Dynamic Shear Results – Test & Analysis (24 Elements Through Diameter)

Table 4. Summary of Dynamic Shear Analysis Results

Duration (ms)	Peak Accel (Gs)	DVRT Failure Time (ms)	Stroke Failure Time (ms)	Percent Difference (%)
0.25	2075	0.276	0.281	1.80%
0.5	1600	0.406	0.354	13.68%
1	1650	0.712	0.513	32.49%
1.5	1675	0.972	0.728	28.71%
2	1650	1.31	0.965	30.33%
2.5	1650	1.5	1.15	26.42%
3	1650	1.82	1.34	30.38%

VI. Discussion and Conclusions

The present study has investigated uncertainties associated with test data acquisition, measurement techniques, analysis simplifications, and mesh sensitivities in order to better understand the error margins an analyst can expect in their similar applications. A comparison of conventional fastener measurement techniques (the stroke displacement) and more local techniques (DVRTs) revealed that compliance can have a significant effect on the acquired test data, and if incorrectly interpreted, models can nonconservatively predict the energy absorption of the joint. These large differences in displacement can then manifest in calibrated models which, when extended to dynamic applications, can lead to errors of approximately 20% (and up to 30%) in common quantities of interest, including failure load, failure time, and displacement at failure. This can have further implications in system models with many fasteners, as these errors and uncertainties can propagate through the model and lead to increasingly poor predictions. Furthermore, the mesh sensitivities of the tensile and shear applications are very different, as the tensile model converged around 4 elements through the diameter while the shear application converged at 24 elements. Therefore, even if local measurement techniques lead to a reliable calibration, the limiting element count of system model analyses make it difficult to exercise a reduced order fastener model that is applicable for both tensile and shear loadings.

Since the analysis of complex structures is dependent on the performance of each component submodel, the procedure of obtaining these submodels is critical to overall model credibility. Although threaded fasteners are a common and important component in many structures, fastener modeling is a difficult process complicated by often overlooked variables, including test data acquisition and limitations on model fidelity. These variables can significantly contribute to the error and uncertainty associated with the model, and this study has begun to quantify this behavior and provide guidance on mitigating these effects. When attempting to capture diverse loadings and loading rates in fasteners through simulation, it becomes necessary to thoroughly exercise and explore test and analysis procedures to ensure the final model is appropriate for the desired application.

Appendix

DVRT Hardening Curve X-Y Pairs

0, 145000
0.008478201, 162632.6
0.016173369, 172632.6
0.021574735, 177332.6
0.024815937, 178932.6
0.028662814, 180832.6
0.031594986, 182194.8711
0.034131674, 183344.7782
0.039334118, 184450.7816
0.044742694, 185600.6071
0.050194856, 186759.6987
0.055698297, 187344.6953
0.06671006, 187929.9513
0.078682377, 188566.259
0.091324593, 188902.214

Failure EQPS: 0.23

Stroke Hardening Curve X-Y Pairs

0, 160000
0.003947063, 171350.1238
0.009906934, 178595.83
0.012468659, 180514.8533
0.015269772, 182184.9241
0.01863253, 183273.252
0.022501482, 184405.1209
0.026199823, 185372.1823
0.029665075, 186278.2942
0.033370309, 187247.158
0.037258939, 187826.2984
0.040895306, 188367.8689
0.050888905, 189451.0904
0.062799183, 190279.2214
0.075758386, 190391.854

Failure EQPS: 0.255

Acknowledgments

Sandia National Laboratories is a multimission laboratory managed and operated by National Technology and Engineering Solutions of Sandia, LLC, a wholly owned subsidiary of Honeywell International, Inc., for the U.S. Department of Energy's National Nuclear Security Administration under contract DE-NA0003525.

References

[1] Mersch, J. P., Smith, J. A., Johnson, E. P., "A CASE STUDY FOR THE LOW FIDELITY MODELING OF THREADED FASTENERS SUBJECT TO TENSILE LOADINGS AT LOW AND HIGH STRAIN RATES," *ASME Pressure Vessels and Piping Conference,* PVP2017-65518, ASME, Waikoloa, HI, 2017.

[2] Fukuoka, T., Nomura, M., "Proposition of Helical Thread Modeling With Accurate Geometry and Finite Element Analysis", *Journal of Pressure Vessel Technology*, Vol. 130, No. 1, 2008, pp. 1-6.

[3] Huang, J., Guo, L., "The Research On the Torque-Tension Relationship for Bolted Joints," *Key Engineering Materials*, Vol. 486, 2011, pp. 242-245.

[4] Zhao, L.B., Liu, F.R., Zhang, J.Y., "3D Numerical Simulation and Fatigue life prediction of high strength threaded bolt," *Key Engineering Materials*, Vol. 417-418, 2010, pp. 885-888.

[5] Grewal, A.S., Sabbaghian, M., "Load distribution between threads in threaded connections," *Journal of Pressure Vessel Technology*, Vol. 119, No. 1, 1997, pp. 91-95.

[6] Majzoobi, G.H., Sadri, A., Bayat, A., Mahmoudi, A.H., "A THREE DIMENSIONAL NUMERICAL STUDY OF STRESS DISTRIBUTION IN BOLT-NUT CONNECTIONS", *Proceedings of the 18th IASTED International Conference, Modelling and Simulation*, 2007, pp. 452-458.

[7] Castelluccio, G.M., Brake, M.R.W., "On the origin of computational model sensitivity, error, and uncertainty in threaded fasteners," *Computers & Structures,* Vol. 186, 2017, pp.1-10.

[8] Bursi, O.S., Jaspart, J.P., "Benchmarks for Finite Element Modelling of Bolted Steel Connections," *Journal of Constructional Steel Research*, Vol. 43, No. 1-3, 1997, pp. 17-42.

[9] Ju, S. –H., Fan, C. –Y., Wu, G.H., "Three-dimensional finite elements of steel bolted connections," *Engineering Structures*, Vol. 26 No. 3, 2004, pp. 403-413.

[10] Fernandez, J., Pernia, A., Martinez-de-Pison, F.J., Lostado, R., "Prediction models for calculating bolted connections using data mining techniques and the finite element method," *Engineering Structures*, Vol 32, No. 10, 2010, pp. 3018-3027.

[11] Knight Jr., N.F., Phillips, D.R., Raju, I.S., "Simulating the Structural Response of a Preloaded Bolted Joint," *49th AIAA/ASME/ASCE/AHS/ASC Structures, Structural Dynamics, and Materials Conference*, AIAA 2008-1842, AIAA, Schaumburg, IL, 2008.

[12] Razavi, H., Abolmaali, A., Ghassemieh, M., "Invisible elastic bolt model concept for finite element analysis of bolted connections", *Journal of Constructional Steel Research*, Vol. 63 No. 5, 2007, pp. 647-657.

[13] Qin, T., Zhao, L, Zhang, J., "Fastener effects on mechanical behaviors of double-lap composite joints", *Composite Structures*, Vol. 100, 2013, pp. 413-423.

[14] Stocchi, C., Robinson, P., Pinho, S. T., "A detailed finite element investigation of composite bolted joints with countersunk fasteners", *Composites Part A - Applied Science and Manufacturing*, Vol. 52, 2013, pp. 143-150.

[15] Fransplass, H., Langseth, M., Hopperstad, O. S., "Tensile behaviour of threaded steel fasteners at elevated rates of strain", *International Journal of Mechanical Sciences,* Vol. 53, No. 11, 2011, pp 946-957.

[16] Fransplass, H., Langseth, M., Hopperstad, O. S., "Numerical study of the tensile behaviour of threaded steel fasteners at elevated rates of strain", *International Journal of Impact Engineering,* Vol. 54, 2013, pp 19-30.

[17] Fransplass, H., Langseth, M., Hopperstad, O. S., "Experimental and numerical study of threaded steel fasteners under combined tension and shear at elevated loading rates", *International Journal of Impact Engineering,* Vol. 76, 2015, pp 118-125.

[18] Egan, B., McCarthy, C. T., McCarthy, M. A., Gray, P.J., O'Higgins, R. M., "Static and high-rate loading of single and multi-bolt carbon-epoxy aircraft fuselage joints", *Composites Part A - Applied Science and Manufacturing*, Vol. 53, 2013, pp. 97-108.

[19] AIA/NAS – Aerospace Industries Association of America Inc., 2016, "English -- SCREW, CAP, SOCKET HEAD, UNDRILLED AND DRILLED, PLAIN AND SELF-LOCKING, ALLOY STEEL, CORROSION-RESISTANT STEEL AND HEAT-RESISTANT STEEL, UNRC-3A AND UNRC-2A - Rev 13", AIA/NAS NAS1352.

[20] Sierra Solid Mechanics Team, "Sierra/SolidMechanics 4.42 User's Guide", Sandia National Laboratories, Albuquerque, NM, 2016. SAND2016-9916.

[21] Smith, Jeff A., Mersch, John P., Hickman, Randy J., Wise, Jack L., "Impact Testing and Analysis of Metal Slugs," SAND2015-4578, Sandia National Laboratories, Albuquerque, NM, 2015

[22] ASME –The American Society of Mechanical Engineers, 2003, "Unified Inch Screw Threads (UN and UNR Thread Form)", ASME B1.1-2003.

[23] *Orient, G. E., Mersch, J. P., "Multilinear Elastic-Plastic Constitutive Calibrations Supporting UQ for Al6061T651, Al7075T651", Sandia National Laboratories, Albuquerque, NM, 2017, SAND Report DRAFT.*

[24] Fastenal Industrial & Construction Supplies, Technical Reference Guide, S7028 Rev. 9, Printed 9/13/2005, https://www.fastenal.com/content/documents/FastenalTechnicalReferenceGuide.pdf

[25] Klopp, W. D., (1987)., High Strength Steel 4140. In Aerospace and High Performance Alloys Database (AHAD), Version 1.6. CINDAS LLC. http://cindasdata.com/

[26] Brown, K. R., (1988)., High Strength Steel 4130. In Aerospace and High Performance Alloys Database (AHAD), Version 1.6. CINDAS LLC. http://cindasdata.com/

[27] Grimmer, P. et. al, "Evaluation of the nonlinear mechanical response in threaded fasteners" *The Conference on Advancing Analysis & Simulation in Engineering*, Cleveland, OH, 2018 (submitted for publication).